

CRYSTAL STRUCTURES OF NATURAL OLIVINES

J. D. BIRLE¹, G. V. GIBBS², P. B. MOORE, AND J. V. SMITH,
*Department of the Geophysical Sciences, University of Chicago
 Chicago, Illinois 60637, U.S.A.*

ABSTRACT

Atomic parameters were obtained by 3D least-squares X-ray diffraction analysis of forsterite ($Mg_{0.90}Fe_{0.10}$), plutonic hyalosiderite ($Mg_{0.535}Fe_{0.456}Mn_{0.006}Ca_{0.002}$), dike hortonolite ($Mg_{0.49}Fe_{0.49}Mn_{0.01}Ca_{0.01}$), and fayalite ($Fe_{0.92}Mg_{0.04}Mn_{0.04}$).

The closeness in value of the isotropic temperature factors calculated for the M sites indicates substitutional disorder of the Mg and Fe atoms in all four structures. Polyhedra distortions are closely similar in all four structures showing that they depend on the structure type rather than on the Mg, Fe substitution. Simple electrostatic rules allied with packing considerations permit qualitative explanation of the structural distortions. The $M(1)$ octahedron has six short shared edges to give a distorted and elongated trigonal antiprism. The $M(2)$ octahedron has a triangle of three short shared edges. Metal-oxygen distances tend to compensate *e.g.*, the longest Si-O distance and the shortest (Mg,Fe)-O distance go to the same oxygen.

INTRODUCTION

The type structure of olivine was determined by Bragg and Brown (1926) on a forsterite crystal with composition $Mg_{0.50}Fe_{0.10}$. Three-dimensional refinement of another forsterite crystal by Belov, Belova, Andrianova, and Smirnova (1951) yielded Si-O and M-O distances far outside the usual ranges for silicates. More recently Hanke and Zemann (1963) determined the atomic parameters of forsterite from a two-dimensional analysis, and Born (1964) followed this by showing that the observed position of $M(2)$ falls on the maximum of the total attractive plus repulsive energy for half-ionized atoms. Hanke (1963) has described a similar two-dimensional analysis of a fayalite crystal. A preliminary description of the present work has already appeared (Gibbs, Moore and Smith, 1964). Geller and Durand (1960) determined the parameters of isostructural lithiophilite, $LiMnPO_4$ and found Li to occupy the smaller $M(1)$ position and Mn the larger $M(2)$ position. Onken (1965) refined the crystal structure of monticellite, $CaMgSiO_4$ and showed that Mg and Ca are ordered in the $M(1)$ and $M(2)$ sites respectively. Caron, Santoro, and Newnham (1965) determined the magnetic structure of glaucochroite, $CaMnSiO_4$, and their neutron diffraction studies showed that this mineral is isomorphous with monticellite.

Sahama and Torgeson (1949) and Bloss (1952) concluded from heats of solution and densities that the olivine system showed ideal substitu-

¹ C.I.C. exchange student from Ohio State University, Department of Mineralogy.

² Present address: Department of Geological Sciences, Virginia Polytechnic Institute.

tion. Yoder and Sahama (1957) from a plot of the spacing of the (130) planes versus composition suggested that the variation of cell parameters with composition did not deviate greatly from Vegard's rule, though Jambor and Smith, C. H. (1964) reported that there is a relatively sharp break from a linear relation of spacing versus composition, and suggested that ordering of Mg and Fe might explain the nonlinear relation. Henriques (1957) gave equations for relating the cell dimensions of olivine to the Mg, Mn and Fe contents. Smith and Stenstrom (1965) have shown that when allowance is made for lattice expansion by Ca and Mn, there is a continuous almost linear, relation between $d(130)$ and atomic percent Mg. Louisnathan and Smith (submitted for publication) have shown that the cell edges have near-linear variations with the atomic fraction of Mg, and have determined the regression coefficients with Mg, Ca and Mn. Lehmann, Dutz and Koltermann (1963) and Duke and Stephens (1964) have shown that there is a linear relation between the Fe content and the absorption frequencies of infrared radiation. Saksena (1961) calculated approximately the positions of the absorption bands for vibrations in this SiO_4 tetrahedron, and Duke and Stephens showed that the multiplicity of the bands was consistent with the symmetry of the potential field.

Contradicting the above evidence for ideal substitution in the olivine structure is the study by Eliseev (1958) who estimated optically the Mg:Fe ratios of several olivines and claimed that the measured cell volumes deviated greatly from Vegard's rule. He suggested that, because the b/c ratio approaches $\sqrt{3}$ as the Fe-content increased, the oxygen atoms in fayalite more nearly approach the ideal configuration of hexagonal close packing than those of forsterite. Similarly he claimed that the forsterite structure becomes more ideal at higher temperatures because of approach of the axial ratio to $\sqrt{3}$. He also observed the presence of extra reflections in the powder patterns of olivine at spacings of 4.703, 4.030, 3.330, and 1.776 Å, which he claimed were the result of "secondary diffraction" in a unit cell with c doubled over the value found by all other workers. Ghose (1962), noting the suggestion of Eliseev that olivine disobeyed Vegard's rule, suggested that the Mg and Fe^{2+} atoms were ordered and by analogy with monticellite, predicted that the larger Fe^{2+} atom would concentrate into the $M(2)$ site occupied by Ca in monticellite.

The present investigation was carried out to resolve the question of ordering, to determine the distortions of the crystal structure and to provide accurate bond lengths as part of a program aimed at understanding the chemical forces in silicates.

EXPERIMENTAL

We are grateful to Professor D. Jerome Fisher, Professor C. E. Tilley, Dr. H. S. Yoder, and Mr. Paul E. Desautels respectively, for supplying forsterite from a nodule from Minas

Gerais, Brazil, hyalosiderite from the Skaergaard intrusion, Kangerdlugssuag, Greenland, hortonolite from a wide dike at Camas Mór, Muck, Scotland and fayalite in lithophysae from Obsidian Cliff, Yellowstone National Park, Wyoming. The forsterite was estimated by optical methods to have a composition near $Mg_{0.90}Fe_{0.10}$. This estimate checks well with estimated compositions by microprobe techniques for other forsterites from inclusions in basaltic rocks (Smith, 1966). In contrast to this homogeneous forsterite, the hortonolite from an olivine gabbro dike in Camas Mór, Muck, Scotland was found to be strongly zoned. Conventional bulk chemical analysis by J. H. Scoon (Tilley, 1952) yielded a composition $Mg_{0.45}Fe_{0.52}Mn_{0.01}Ca_{0.01}$; however the large amount of Al and Fe^{+3} casts doubt on the applicability of the analysis to the olivine. Microprobe analysis of the single crystal used for collection of diffraction data yielded a composition $Mg_{0.49}Fe_{0.49}Mn_{0.01}Ca_{0.01}$. The hyalosiderite from the Skaergaard intrusion corresponds to sample YS-15 in Smith (1966) and the composition $Mg_{0.536}Fe_{0.456}Mn_{0.006}Ca_{0.002}$ obtained by microprobe analysis was adopted. Fayalite was found to be zoned by electron microprobe techniques affording an average composition $Mg_{0.039}Fe_{0.922}Mn_{0.037}Ca_{0.002}$ and ranges of Mg 0.00 to 0.08 and of Mn 0.03 to 0.04. Cell dimensions were estimated from plots of cell dimensions *vs* composition obtained from data by Louisnathan and Smith (submitted for publication). The consistency of the data indicate that the cell dimensions are accurate to about 1 in 1000. We chose forsterite, *a* 4.762, *b* 10.225, *c* 5.994; dike hortonolite, *a* 4.787, *e* 10.341, *c* 6.044; plutonic hyalosiderite *a* 4.785, *b* 10.325, *c* 6.038; and fayalite, *a* 4.816, *b* 10.469, *c* 6.099 Å.

Long-exposure single crystal X-ray photographs showed the Laue symmetry and systematic absences for the space group *Pbnm*. Eliseev's suggestion of double diffraction from a superstructure cannot be valid because the intensities of the extra reflections would be far too weak to be observed in his powder photographs. Unsuccessful attempts were made to explain the reflections on the basis of target contamination in the X-ray tube or of contamination of the sample. Unless confirmation is obtained of Eliseev's extra reflections, it seems safe to assume that all olivine crystals obey the symmetry of *Pbnm* and have the normal cell size.

Intensities for the forsterite, hyalosiderite and hortonolite were collected for each crystal using a manual Weissenberg equi-inclination counter diffractometer with moving crystal and fixed scintillation counter. The fayalite data were gathered automatically on a PAILRED unit. Monochromatized $MoK\alpha$ radiation was used for all four crystals and the polarization effect of the monochromator was ignored in applying the Lorentz and polarization factors. 2026 independent intensities were gathered for fayalite but 308 were omitted because of asymmetrical backgrounds and 304 because of indistinguishability from background. Nonspherical absorption corrections were applied to forsterite, but were not needed for the other three because of favorable shape and small size of the crystals.

Full matrix isotropic least-squares refinements were made using the Busing-Martin-Levy ORFLS program. The atomic form factor curves were taken from Berghuis *et al.*, (1955) and from Freeman (1959) after arbitrary modification for half-ionization. For the two octahedral sites, an average curve was prepared assuming complete disorder.

Any ordering of the octahedrally-coordinated atoms would be revealed by unequal temperature factors for the two sites. Initial refinements of the forsterite data indicated extinction effects for the strong reflections and about eighty reflections were omitted from the final refinements. No such effect was noticed for the hyalosiderite and hortonolite and all reflections were given equal weight during the refinement. For fayalite extinction was small but thirty of the strongest reflections were omitted. The number of independent reflections used in the final refinements was as follows: forsterite (414), dike hortonolite (367), plutonic hyalosiderite (924), and fayalite (1384).

The final isotropic temperature factors for these four olivines are comparable with those from similar structure types, and the factors for the two octahedral sites are consistent with disorder of the Mg and Fe atoms. Because of the large difference between the scatter-

ing factors for Mg and Fe, errors in the Mg and Fe contents applied to the sites would have a strong influence on the estimated temperature factors. An estimate of the effect was obtained by using separate scattering factor curves for Fe and Mg in place of the averaged curves. Applying Mg to the $M(1)$ site and Fe to the $M(2)$ site of hortonolite gave in the first cycle of refinement temperature factors of -4.9 and $+5.0$ for the two octahedral sites. Thus, an error of 1 percent in the Mg:Fe ratio of the hortonolite and hyalosiderite would shift the temperature factors of the octahedral sites by about 0.1. The range of B values between the four structures could be accounted for merely by errors in the composition (average B : Fo 0.34, Hy 0.35, Ho 0.41, Fa 0.38); indeed the argument may be reversed to claim that the listed Mg and Fe compositions are accurate to 0.01 in spite of the difficulty of analyzing zoned crystals.

Table 1 lists the atomic parameters and their standard errors, Table 2 the interatomic distances and Table 3¹ the observed and calculated structure amplitudes. The final discrepancy factors for reflections used in isotropic refinements are 0.08 for forsterite, 0.07 for dike hortonolite, 0.08 for plutonic hyalosiderite and 0.07 for fayalite. A three-cycle anisotropic refinement for fayalite rapidly converged to $R=0.05$ and yielded apparently significant deviations from spherical symmetry of the ellipsoids: however, these deviations will not be discussed at this time because the effect of differential absorption has not been evaluated in detail.

DISCUSSION

The idealized olivine structure (Fig. 1a) consists of a hexagonal close-packed array of oxygen atoms in which one-half of the available octahedral voids are occupied by M atoms and one-eighth of the available tetrahedral voids by Si atoms. To enumerate all the possibilities of arranging atoms in the voids is beyond the scope of the present paper but will be pursued elsewhere because of its importance. For example, there are several recently-determined structures which have metal atoms occupying the voids in hexagonally close-packed oxygen atoms. In particular, welinite, recently determined by Moore (in preparation) has the properties $Mn_7Si_2O_{14}$, a 8.155, c 4.785 Å, $P6_3$: here half of the octahedral voids are occupied but only one-fourteenth of the tetrahedral voids. This arrangement is shown idealized in Fig. 1b. An interesting arrangement with the olivine stoichiometry M_2TO_4 is shown in Figure 1c. The relations to hypothetical structures based on occupancy of voids in cubic close packed oxygen atoms (such as in spinel and kyanite) are also of interest, especially in view of the pressure dependence of transitions such as the well-known olivine-spinel transition.

Returning to the olivine structure it may be seen from Figure 1a that the key structural unit is the serrated chain of octahedra lying parallel to the z -axis. In any one yz layer only half the octahedral voids are oc-

¹ Table 3 has been deposited as Document No. 9901 with the American Documentation Institute, Auxiliary Publications Department, Photoduplication Service, Library of Congress, Washington, D.C. 20420. Copies may be secured by citing the document number and remitting in advance \$3.75 for photoprints or \$2.00 for microfilm.

TABLE 1. ATOMIC PARAMETERS

Atom	Forsterite				Hyalosiderite (Skaergaard)			
	<i>x</i>	<i>y</i>	<i>z</i>	<i>B</i>	<i>x</i>	<i>y</i>	<i>z</i>	<i>B</i>
<i>M</i> (1)	0	0	0	0.33(3)	0	0	0	0.32(1)
<i>M</i> (2)	0.98975(29)	0.27743(16)	$\frac{1}{4}$	0.36(3)	0.98598(21)	0.27880(17)	$\frac{1}{4}$	0.37(2)
Si	.42693(27)	.09434(13)	$\frac{1}{4}$	0.20(3)	.42843(25)	.09587(22)	$\frac{1}{4}$	0.19(2)
O(1)	.76580(72)	.09186(36)	$\frac{1}{4}$	0.35(5)	.76566(60)	.09430(53)	$\frac{1}{4}$	0.40(4)
O(2)	.22012(72)	.44779(36)	$\frac{1}{4}$	0.42(5)	.21642(73)	.45084(55)	$\frac{1}{4}$	0.56(5)
O(3)	.27810(50)	.16346(25)	.03431(46)	0.41(5)	.28264(46)	.16370(4)	.03435(55)	0.50(3)
	Hortonolite (Camas M6r)				Fayalite			
<i>M</i> (1)	0	0	0	0.36(4)	0	0	0	0.41(1)
<i>M</i> (2)	.98678(23)	.27915(12)	$\frac{1}{4}$	0.47(4)	.98608(13)	.28004(6)	$\frac{1}{4}$	0.36(1)
Si	.42870(35)	.09576(14)	$\frac{1}{4}$	0.18(5)	.43070(25)	.09723(11)	$\frac{1}{4}$	0.27(1)
O(1)	.76844(92)	.09173(39)	$\frac{1}{4}$	0.28(7)	.76683(63)	.09197(29)	$\frac{1}{4}$	0.43(3)
O(2)	.21419(79)	.44958(37)	$\frac{1}{4}$	0.18(6)	.21027(66)	.45308(30)	$\frac{1}{4}$	0.48(3)
O(3)	.28401(61)	.16395(26)	.03442(48)	0.37(6)	.28806(45)	.16532(21)	.03626(43)	0.52(2)

TABLE 2. INTERATOMIC DISTANCES (Å) IN OLIVINE

Atoms	Forsterite	Hyalosiderite(S)	Hortonolite(CM)	Fayalite
<i>Si tetrahedron</i>				
1 Si -O(1)	1.614(4)	1.613(3)	1.627(7)	1.619(2)
1 -O(2)	1.654(4)	1.650(6)	1.659(6)	1.657(2)
2 -O(3)	1.635(3)	1.634(3)	1.636(4)	1.637(2)
mean	1.634	1.634	1.639	1.638
1 O(1) -O(2)	2.743(5)	2.740(6)	2.738(9)	2.723(3)
2 -O(3)	2.757(4)	2.747(4)	2.763(7)	2.759(3)
2 O(2) -O(3) ^a	2.556(4)	2.554(6)	2.571(6)	2.575(3)
1 O(3) -O(3) ^a	2.586(6)	2.603(5)	2.606(8)	2.605(4)
mean	2.659	2.658	2.669	2.666
<i>M(1) octahedron</i>				
2 M(1)-O(1)	2.091(2)	2.116(3)	2.100(4)	2.125(2)
2 -O(2)	2.075(2)	2.091(5)	2.104(4)	2.123(2)
2 -O(3)	2.142(3)	2.174(3)	2.183(4)	2.228(2)
mean	2.103	2.127	2.129	2.159
2 O(1) -O(2) ^b	2.857(5)	2.886(6)	2.880(9)	2.906(3)
2 -O(2)	3.032(1)	2.062(1)	3.063(1)	3.098(1)
2 -O(3) ^b	2.857(4)	2.885(4)	2.889(7)	2.928(3)
2 -O(3)	3.125(4)	3.177(6)	3.164(7)	3.222(3)
2 O(2) -O(3) ^a	2.556(4)	2.554(6)	2.571(6)	2.575(4)
2 -O(3)	3.355(4)	3.417(4)	3.431(7)	3.508(4)
mean	2.964	2.997	3.000	3.039
<i>M(2) octahedron</i>				
1 M(2)-O(1)	2.177(4)	2.177(5)	2.202(6)	2.232(2)
1 -O(2)	2.059(4)	2.090(3)	2.071(6)	2.110(2)
2 -O(3)	2.217(3)	2.262(3)	2.267(4)	2.291(2)
2 -O(3)	2.070(3)	2.060(3)	2.060(4)	2.072(2)
mean	2.135	2.152	2.154	2.178
2 O(1) -O(3) ^b	2.857(4)	2.886(4)	2.880(7)	2.906(3)
2 -O(3)	3.028(4)	3.032(1)	3.057(6)	3.084(3)
2 O(2) -O(3)	3.194(4)	3.253(6)	3.246(6)	3.303(3)
2 -O(3)	2.937(4)	2.940(4)	2.928(6)	2.956(3)
1 O(3) -O(3) ^a	2.586(6)	2.603(5)	2.606(8)	2.605(4)
2 -O(3)	3.408(6)	3.432(5)	3.438(8)	3.494(3)
2 -O(3)	2.995(3)	3.011(5)	3.011(5)	3.024(2)
mean	3.001	3.023	3.024	3.054

TABLE 2—(Continued)

Atoms	Forsterite	Hyalosiderite(S)	Hortonolite(CM)	Fayalite
<i>O(1) bonds</i>				
1 O(1) -Si	1.614(4)	1.613(3)	1.627(7)	1.619(2)
2 -M(1)	2.091(2)	2.116(3)	2.100(4)	2.125(2)
1 -M(2)	2.177(4)	2.177(5)	2.202(6)	2.232(2)
<i>O(2) bonds</i>				
1 O(2) -Si	1.654(4)	1.650(6)	1.659(6)	1.657(2)
2 -M(1)	2.075(2)	2.091(3)	2.104(4)	2.123(2)
1 -M(2)	2.059(4)	2.090(3)	2.071(6)	2.110(2)
<i>O(3) bonds</i>				
1 O(3) -Si	1.635(3)	1.634(3)	1.636(4)	1.637(2)
1 -M(1)	2.142(3)	2.174(3)	2.183(4)	2.228(2)
1 -M(2)	2.217(3)	2.262(3)	2.267(4)	2.291(2)
1 -M(2)	2.070(3)	2.060(3)	2.060(4)	2.072(2)

^a edges shared between tetrahedron and octahedron

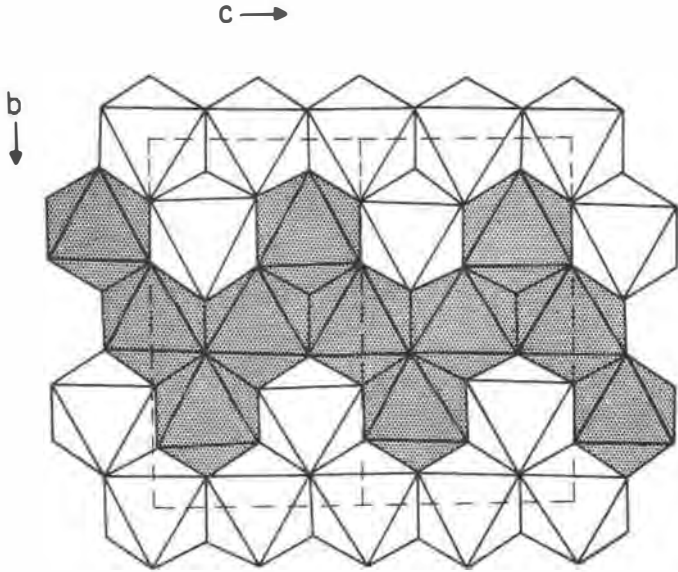
^b edges shared between octahedra

Numbers in parentheses are standard errors. The number preceding an atom designation is the multiplicity of the second atom with respect to the first.

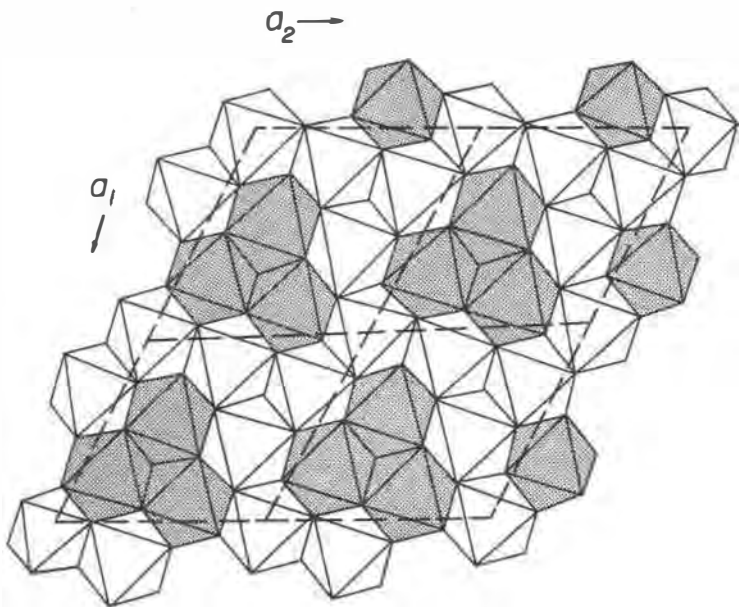
Note that the error does not include the effect of error in the cell dimensions.

cupied resulting in a serrated chain of unoccupied octahedra whose shape is the same as that of the occupied band, but which is displaced $b/2$ (see also Fig. 2). The next layer of occupied octahedra is displaced $a/2$ from the first layer. The occupied serrated chain lies directly above the unoccupied serrated chain of the first layer, and is related to the occupied chain of the first layer by the b glide plane. Accordingly, none of the octahedra share faces in common. The serrated chains are joined together by silicon-centered tetrahedra which share a triangle of edges with octahedra from one serrated chain and which share the vertex opposing the triangle with a vertex from each of three octahedra belonging to a serrated chain displaced a away from the first chain. In contrast to the chains from alternate layers which are linked by this edge and vertex sharing with silicate tetrahedra, chains of adjacent layers are linked by vertex sharing of octahedra. The implied importance of the serrated chain lying parallel to z is consistent with the two observed cleavages $\{100\}$ and $\{010\}$ and the occurrence of $\{h\bar{h}0\}$ as dominant forms.

Perhaps the most interesting structural feature is the extreme distortion of the polyhedra even though the structure is based on a close-packed arrangement of oxygen atoms. Although covalent forces undoubtedly contribute, the principal features of the distortions can be explained by the application of Pauling's rules based on simple electrostatic forces.



(a)



(b)

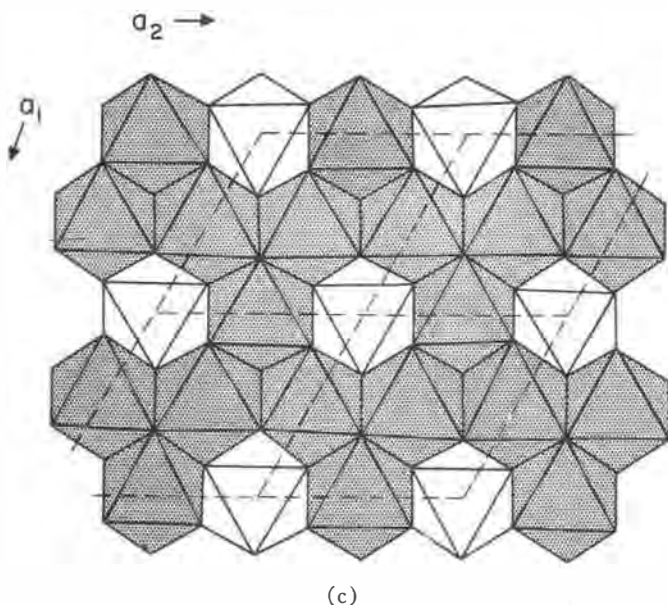


FIG. 1. Octahedral populations in the crystal structures of (a) olivine, (b) welinite, and (c) a hypothetical structure with olivine stoichiometry. Shaded and unshaded octahedra distinguish the two levels normal to the plane of the drawings.

These predict a shortening of shared edges and a lengthening of cation-bonds to oxygen atoms of shared edges because of cation-cation repulsion.

The principal distortions do indeed correlate with the sharing of polyhedral edges. From Table 2 it may be seen that the distortions are essentially the same in all four structures and that substitution of Mg for Fe has little effect. In the following part of the discussion and in the figures distances averaged over the forsterite and hortonolite will be used.

From Figure 3 it may be seen that the silicon tetrahedron is almost a trigonal pyramid elongated parallel to the x -axis. The $M(1)$ octahedron which lies on an inversion center approximates to a trigonal antiprism because of the two opposing triangles of short shared edges. However the shared edges vary by 0.3 \AA as do the unshared edges so the approximation to an antiprism is poor. The $M(2)$ octahedron cannot be approximated by any symmetrical polyhedron: the triangle of short shared edges is the most important feature: it should be noted that the point symmetry of $M(2)$ is C_v .

The cation-oxygen distances cannot be interpreted simply but there are some crude relationships. From Table 2 it may be seen that each

oxygen is bonded to one Si and three M atoms. The longest Si-O distance is to O(2) which has the shortest M-O distances. In the $M(2)$ octahedron and the Si tetrahedron (Fig. 3) the longest bonds are to oxygens forming the shared edges (2.19 and 2.24 vs. 2.06 and 2.07; 1.63 and 1.65 vs. 1.62 Å). In the $M(1)$ octahedron all the oxygens belong to shared edges and the distances 2.09, 2.09 and 2.16 are more regular than those in $M(2)$. Thus the lengthening of cation bonds to shared oxygens explained by Pauling as the result of cation-cation repulsion is displayed nicely in olivine.

As might be expected from the greater charge on the silicon ion, the edges shared between a tetrahedron and an octahedron (2.56 and 2.60 Å) are shorter than those shared between octahedra (2.87 and 2.89 Å). Unshared edges are all larger than the shared edges in the same polyhedron: Si tetrahedron, 2.73 and 2.76; octahedra, 2.94 to 3.44 Å. Although the shared edges are shorter than the unshared edges, the great variation in the lengths of the unshared edges in the octahedron shows that the situation is actually more complex. Comparison of Figure 3c with Figure 2b shows that shortening of the O(3)-O(3) edge shared between the $M(2)$ and Si polyhedra results in a lengthening of the other O(3)-O(3) edge which lies parallel to the z -axis: this arises because these two O(3)-O(3) edges add up to yield the c repeat distance which is not completely free to shorten upon sharing of the first edge because of the geometrical requirements of the $M(1)$ octahedra. Indeed comparison of Figure 3b with Figure 2b shows that the c repeat distance is also determined in part by the O(1)-O(2) edges of two $M(1)$ octahedra. These edges are the shortest of the unshared edges of the $M(1)$ octahedron. Thus one can envisage a compromise between conflicting electrostatic and spatial factors such that the first O(3)-O(3) edge shortens and the second one lengthens while the two O(1)-O(2) edges shorten somewhat. Of course a detailed analysis would require simultaneous consideration of all the edges: perhaps such an analysis will become feasible in the future.

Burnham (1963) on the basis of a study of aluminosilicates concluded that "in many cases the minimum-energy configuration of a structure is not primarily dictated by edge-sharing considerations". In olivine, the range of lengths of unshared edges for the M polyhedra is comparable to the difference between the average shared and the average unshared edge. Thus the simple concept of edge sharing would account for about half of the length variations. Born (1964) on the basis of various simplifying assumptions including the positions of the Si and O atoms has been able to predict the position of $M(2)$. Perhaps the safest conclusion at this time is that while Pauling's rules give a simple qualitative explanation of

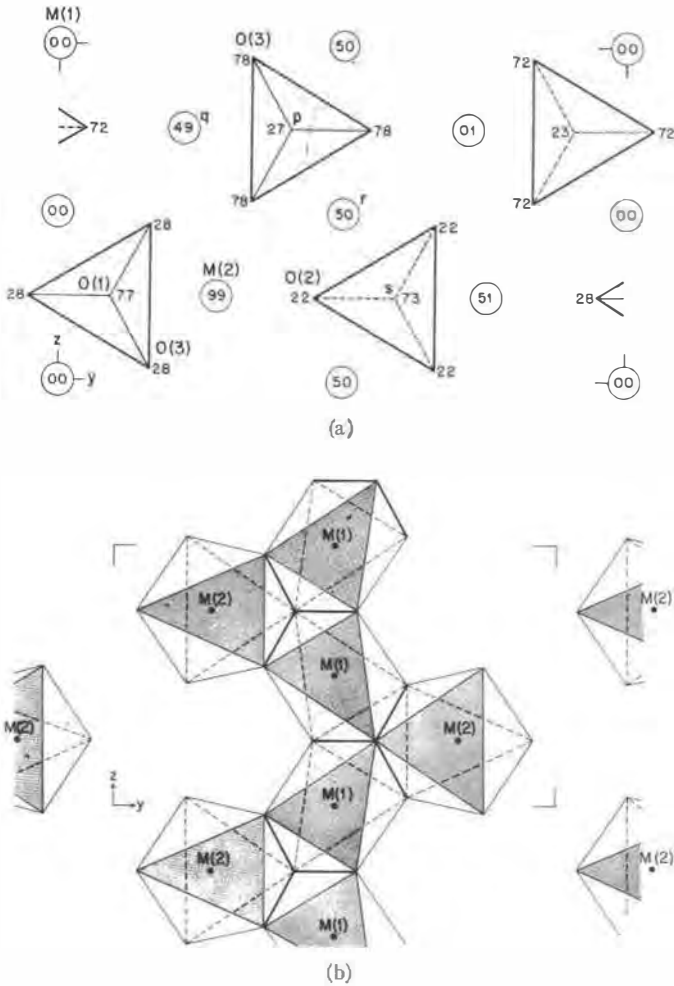
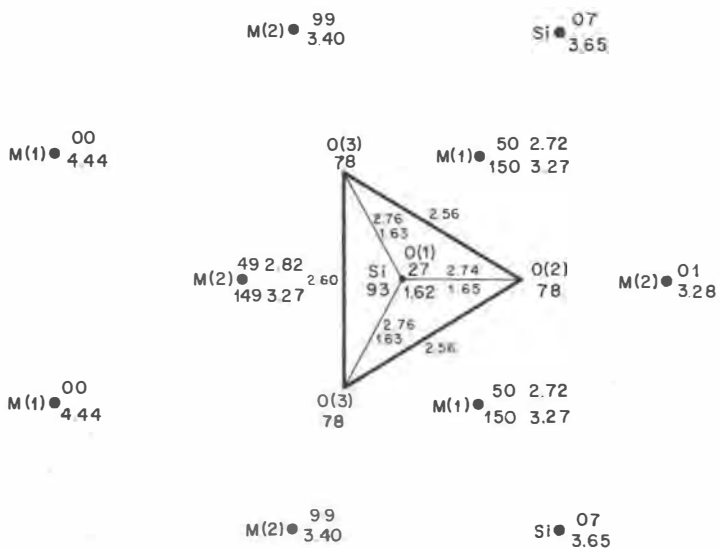
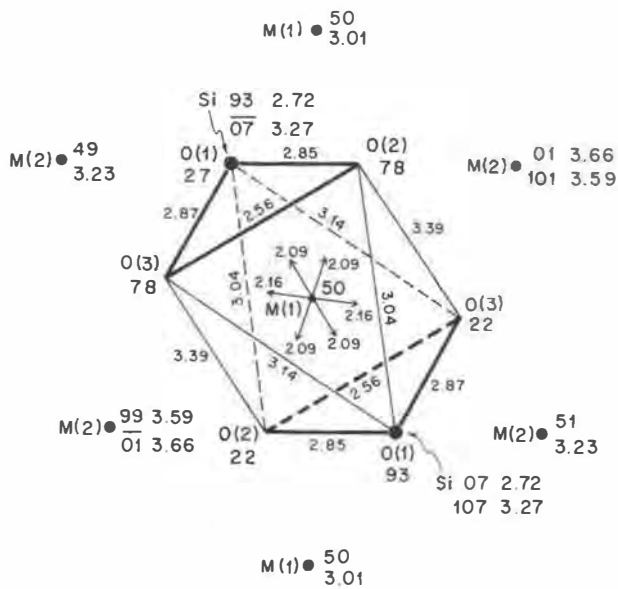


FIG. 2. *a*. Tetrahedral arrangements and the neighboring octahedral sites. Distances along x are given in fractional units. *b*. Actual distortions observed for olivine in a portion of an octahedral serrated band.

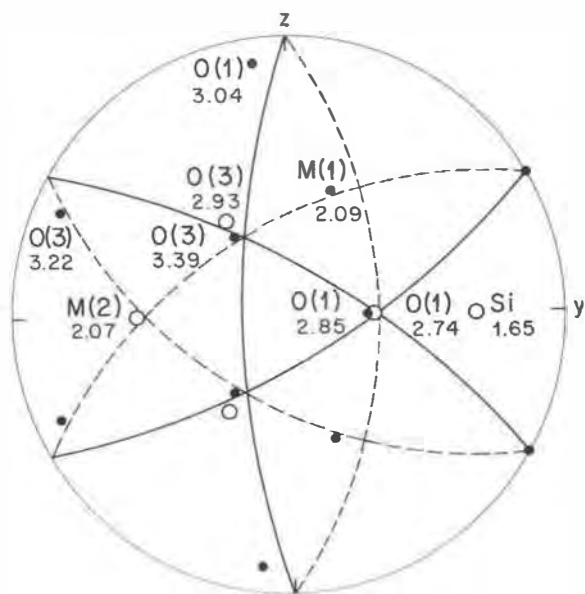
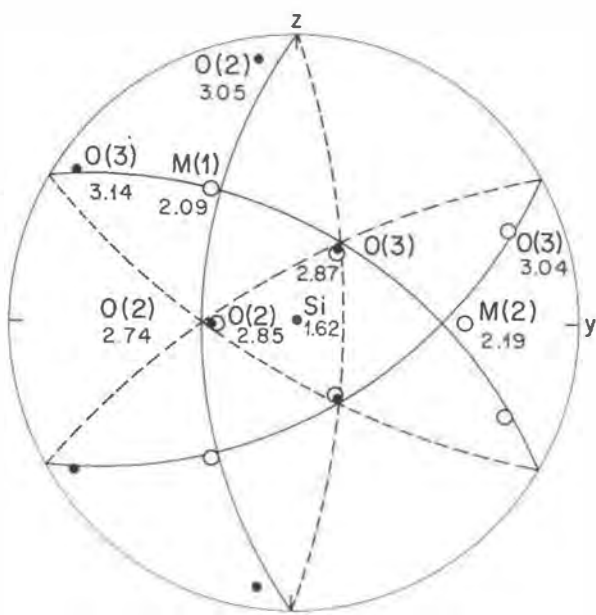
polyhedral distortions, and appear to give a simple semi-quantitative explanation, a rigorous test of the applicability of electrostatic interaction between deformable spheres is too daunting. Perhaps further extension of the approach used by Born with gradual abandonment of the simplifying assumptions might be possible, especially with the developing ease of sequential calculations.



(a)



(b)



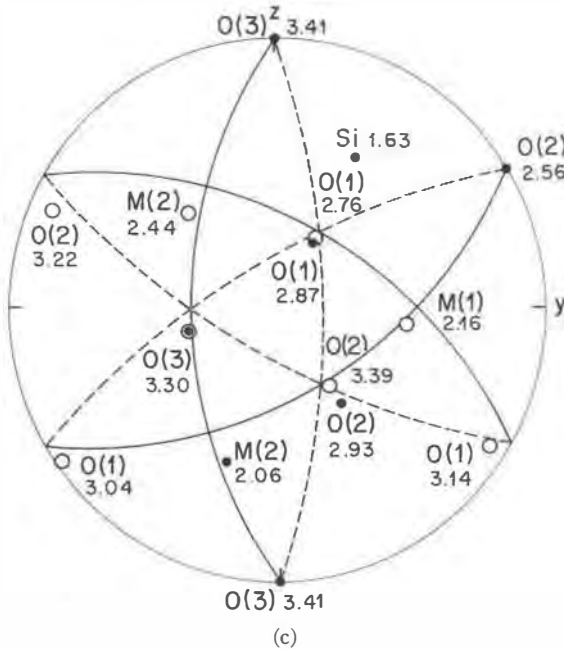


FIG. 5. Stereographic projections of first and second nearest neighbors of oxygen atoms in olivine (a), (b) and (c). About O(1), O(2), and O(3) respectively in olivine. Interatomic distances are given. O = octahedral site, T = tetrahedral site.

Figure 5 is an alternative way of displaying the distortion in the olivine structure (again based on an average of forsterite and hortonolite). Each of the subdiagrams is a stereographic projection of the first and second neighbors of oxygen atoms, the former being tetrahedrally or octahedrally-coordinated atoms, the latter being oxygen atoms. Diagrams (a) and (b) in Figure 4 refer to regular hexagonal and cubic close-packing, respectively; (a) (b) and (c) in Figure 5 refer to O(1), O(2) and O(3) in olivine. It may be seen that only one-eighth of the tetrahedral voids, and one-half of the octahedral voids are occupied.

Comparison of the four structures in terms of increasing Fe content shows that most distances in the hyalosiderite and the hortonolite are intermediate between those of forsterite and fayalite. The $M(1)$ and $M(2)$ octahedra increase considerably in size with entry of the larger Fe ions. The octahedra become more irregular as the Fe content increases, and in contradiction to Eliseev's suggestion, fayalite is more distorted from regular close-packing than is forsterite. The SiO_4 tetrahedron was found to be larger in fayalite but the increase is not significant in terms of

the errors. The Si-O distances fall within the expectations listed by Smith and Bailey (1963): it is worth noting that the average distance in olivine, 1.636, is greater than those for the two tetrahedra in kyanite, 1.623 and 1.633 Å, which is based on cubic close packing, (Burnham, 1963). The average distance in monticellite, 1.624 Å, Onken (1965), is smaller than in the forsterite-fayalite structures. This confirms earlier indications that the mean Si-O distances depends on the nature of other cations and the structure type as well as on the degree of polymerization of the Si-O group.

The surprising aspect of olivine is the absence of evidence for ordering of the octahedral cations in Mg, Fe olivines. Of course, the minor cations such as Ca and Mn cause some complication and it is possible that they occupy one site preferentially. In monticellite (Onken, 1965) magnesium occupies $M(1)$ preferentially: perhaps the larger B value of $M(1)$ in fayalite results from preferential occupancy by Mg. For the other three structures $M(2)$ has the larger B value which might be taken to indicate preferential occupancy by Mg. However it is thought that a larger B value would be expected for $M(2)$ in comparison with $M(1)$ because of the greater irregularity of the $M(2)$ oxygen polyhedron: indeed, preferential occupancy of $M(2)$ by Mg and of $M(1)$ by Fe seems unlikely from a crystal chemical view-point since the larger Fe ion should prefer the larger $M(2)$ polyhedron if a preference does indeed occur. Lack of ordering is consistent with the other physical evidence for near-ideal solid solution summarized in the introduction. That lack of ordering is a surprise results from comparison with orthopyroxene where the two octahedra probably have less distortion than the ones in olivine but in which strong ordering occurs (Ghose, 1962). Slow cooling should have occurred in the Skaergaard intrusion, while even the olivine from the Camas Mór olivine gabbro dike (30 yards across) should have received some opportunity for annealing. Volcanic orthopyroxenes are partly ordered (Hafner, pers. comm.). Presumably there is some key difference between the crystal structures: the near close packed structure of olivine may inhibit movement of octahedral cations more than the less closely-packed structure of pyroxene. Perhaps preferential occupancy in olivine becomes stable thermodynamically only at temperatures too low for effective ionic migration: the frequent occurrence of orthoclase in plutonic and metamorphic rocks shows how difficult is the ordering of Al and Si in K-feldspar.

The present study was begun because of literature reports of anomalous properties in olivine that suggested that parameters might depend on petrologic history and hence serve as petrogenic indicators. Actually the structural parameters are quite regular and apparently immune to

crystallization history. Only the chemical parameters seem to be of value. Perhaps some more subtle structural indicators, for example lamellae may be found of value. In the meantime, the olivine structure serves as an excellent example of the distortions consequent on the stuffing of close-packed oxygen arrays.

ACKNOWLEDGEMENTS

This work was supported by NSF grants G-14467, GP-443, and GA-572. P. B. Moore held an NSF Predoctoral Fellowship during the early stages of this work.

REFERENCES

- BELOV, N. V., E. N. BELOVA, N. H. ANDRIANOVA, AND P. F. SMIRNOVA (1951) Determination of the parameters in the olivine (forsterite) structure with the harmonic three-dimensional synthesis. *Dokl. Akad. Nauk S.S.S.R.*, **81**, 399-402.
- BERGHUIS, J., I. M. HAANAPPEL, M. POTTERS, B. O. LOOPSTRA, C. H. MACGILLAVRY, AND A. L. VEENENDAAL (1955) New calculations of atomic scattering factors. *Acta Crystallogr.*, **8**, 478-483.
- BLOSS, F. D. (1952) Relationship between density and composition in mol percent for some solid solution series. *Amer. Mineral.*, **37**, 966-980.
- BORN, L. (1964) Eine "gitterenergetische Verfeinerung" der freien Mg-Position im Olivin. *Neues Jahrb. Mineral. Monatsh.*, 81-94.
- BRAGG, W. L. AND G. B. BROWN (1926) Die Struktur des Olivins. *Z. Kristallogr.*, **63**, 538.
- BURNHAM, C. W. (1963) Refinement of the crystal structure of kyanite. *Z. Kristallogr.*, **118**, 5/6, 337-360.
- CARON, L. G., R. P. SANTORO, AND R. E. NEWNHAM (1965) Magnetic structure of CaMn SiO₄. *J. Phys. Chem. Solids*, **26**, 927-930.
- DUKE, D. A. AND J. D. STEPHENS (1964) Infrared investigations of the olivine group minerals. *Amer. Mineral.*, **49**, 1388-1406.
- ELISEEV, E. N. (1958) New data on the crystal structure of olivine. *Kristallografiya*, **3**, [Transl. *Sov. Phys.-Crystallogr.* 163-170].
- FREEMAN, A. J. (1959) Atomic scattering factors for spherical and aspherical charge distributions. *Acta Crystallogr.* **12**, 261-271.
- GELLER, S. AND J. L. DURAND (1960) Refinement of the structure of LiMnPO₄. *Acta Crystallogr.*, **13**, 325-331.
- GHOSE, S. (1962) The nature of Mg⁺²-Fe⁺² distribution in some ferromagnesian silicate minerals. *Amer. Mineral.*, **47**, 388-394.
- GIBBS, G. V., P. B. MOORE, AND J. V. SMITH (1964) Crystal structures of forsterite and hortonolite varieties of olivine. *Geol. Soc. Amer. Spec. Pap.*, **76**, 66.
- HANKE, K. (1963) Verfeinerung der Kristallstruktur des Fayalits von Bad Harzburg. *Neues Jahrb. Mineral. Monatsh.*, 192-194.
- AND J. ZEMANN (1963) Verfeinerung der Kristallstruktur von Olivin. *Naturwissenschaften*, **3**, 91-92.
- HENRIQUES, Å (1957) The effect of cations on the optical properties and cell dimensions of knebelite and olivine. *Ark. Mineral. Geol.*, **2**, No. 17, 305-313.
- JAMBOR, J. L. AND C. H. SMITH (1964) Olivine composition determination with small diameter x-ray powder cameras. *Mineral. Mag.*, **33**, 730-741.
- LEHMANN, H., H. DUTZ, AND M. KOLTERMANN (1963) Investigations of the crystalline solid-solution series forsterite-fayalite by infrared spectrography. *Budapest, Akad. Kiadó*, 273-277.

- ONKEN, H. (1965) Verfeinerung der Kristallstruktur von Monticellit. *Tschermak's Mineral. Petrogr. Mitt.*, **10**, 34-44.
- SAHAMA, TH. G. AND D. R. TORGESON (1949) Thermochemical study of the olivines and orthopyroxenes. *U.S. Bur. Mines Rep. Invest.* **4408**, 1-24.
- SAKSENA, B. D. (1961) Infra-red absorption studies of some silicate structures. *Trans. Faraday Soc.* **57**, 242-258.
- SMITH, J. V. AND S. W. BAILEY (1963) Second review of Al-O and Si-O tetrahedral distances. *Acta Crystallogr.*, **16**, 801-811.
- AND R. C. STENSTROM (1965) Chemical analysis of olivines by the electron microprobe. *Mineral. Mag.*, **34**, No. 268, 436-459.
- (1966) X-ray emission microanalysis of rock-forming minerals II: Olivines. *J. Geol.*, **74**, No. 1, 1-16.
- TILLEY, C. E. (1952) Some trends of basaltic magma in limestone syntexis. *Amer. J. Sci.*, Bowen Vol, 529-545.
- YODER, H. S. AND TH. G. SAHAMA (1957) Olivine x-ray determinative curve. *Amer. Mineral.* **42**, 475-491.

Manuscript received, August 8, 1967; accepted for publication, October 13, 1967.